Strong coupling and hybridization of Frenkel and Wannier-Mott excitons in an organic-inorganic optical microcavity

R. J. Holmes,[1,*] S. Kéna-Cohen,[1] V. M. Menon,[2] and S. R. Forrest[3,†]

[1]*Princeton Institute for the Science and Technology of Materials (PRISM), Department of Electrical Engineering, Princeton University, Princeton, New Jersey 08544, USA*

[2]*Department of Physics, Queens College of the City University of New York (CUNY), Flushing, New York 11367, USA*

[3]*Department of Electrical Engineering and Department of Computer Science, Physics, and Materials Science and Engineering, University of Michigan, Ann Arbor, Michigan 48109, USA*

We demonstrate strong exciton-photon coupling and photon-mediated hybridization between the Frenkel and Wannier-Mott excitons of an organic-inorganic hybrid optical microcavity. Hybridization occurs between the Frenkel excitons of the small molecular weight organic tetraphenylporphyrin and the Wannier-Mott excitons of InGaP quantum wells. This mixed state consists of 10% Frenkel and Wannier-Mott exciton and 80% cavity photon character, and persists up to temperatures of 100 K.

I. INTRODUCTION

The absorption of light in a semiconductor can lead to the creation of a bound electron-hole pair, known as an exciton. Frenkel-type excitons are commonly found in organic semiconductors and have large binding energies (~ 1 eV) and small Bohr radii (~ 1 nm). In contrast, W annier-Mott excitons are associated with inorganic semiconductors and are weakly bound (~ 10 meV) with large Bohr radii (~ 10 nm). An exciton placed in an optical microcavity can interact with the photon mode of the cavity.[1] If the resonance leads to a splitting (anticrossing) between the coupled exciton and cavity-photon eigenstates, the system is identified as "strongly coupled."[2] Furthermore, when multiple excitons of a single type (either Frenkel or Wannier-Mott) are confined within the microcavity, they may hybridize by each strongly coupling to the cavity photon field.[3–7] The eigenstates of the strongly coupled exciton-photon system are called microcavity polaritons.[2,8]

Microcavity polaritons were first reported in inorganic (GaAs-based) semiconductor structures at low temperature.[2] Observations of the strongly coupled state are generally limited to low temperature in inorganic materials as a result of thermal linewidth broadening and the small Wannier-Mott oscillator strength. In contrast, the study of strong coupling in organic materials has only recently received attention. Organic materials are interesting in this context due to their large exciton oscillator strengths and binding energies. These properties lead to a stronger interaction with the cavity mode, and a stable, strongly coupled state at room temperature. Strong coupling has been reported in a variety of spun-cast and solution-processed organic materials,[9–13] as well as in thermally evaporated thin films.[4,14]

When multiple excitonic resonances are coupled using a single cavity mode, the excitons are said to be hybridized (or mixed). In inorganic semiconductors, exciton hybridization has been explored by coupling quantum wells of varying thicknesses to a cavity,[6] and also by simultaneously coupling the light and heavy-hole excitonic transitions of a single quantum well (QW) to a common cavity photon mode.[15]

Hybridization has been observed in organic materials between detuned molecular absorbers in a cavity,[5,16] and between the neighboring vibronic transitions of a single molecular material.[4]

In addition, the existence of a hybrid Frenkel/Wannier-Mott polariton state has been predicted theoretically and is expected to exhibit unique nonlinear optical properties.[17,18] The study of hybrid cavity polaritons can also lead to an improved understanding of energy transfer between semiconductor systems with vastly different properties. However, to our knowledge, prior to this work there has not been an experimental demonstration of hybridization between the Frenkel exciton resonance of an organic material and the Wannier-Mott exciton resonance of an inorganic QW. In contrast to earlier work with polaritonic states, this state would involve the coupling of two fundamentally different excitonic oscillators.

Here, we provide evidence for coupling between an exciton in tetraphenylporphyrin (TPP), a red absorbing, small molecular weight organic material, and that in the QWs of $In_{0.52}Ga_{0.48}P$ via a common optical cavity mode. The poor intermolecular overlap present in small molecular weight organic materials such as TPP leads to the formation of Frenkel excitons upon optical excitation. In a Group III–V inorganic semiconductor such as InGaP, optical excitation leads to the formation of highly delocalized Wannier-Mott excitons due to the large-scale order and periodicity of the crystal lattice.

This paper is organized as follows. Section II contains the experimental details describing the fabrication of various microcavity structures. The experimental results are presented in Sec. III. The theoretical framework for interpreting the results followed by a discussion of the results is given in Sec. IV. Conclusions are presented in Sec. V.

II. EXPERIMENTAL

The device structure is shown in Fig. 1 and consists of two optically active semiconductor regions (an InGaP QW structure and a film of the fluorescent organic TPP) sandwiched between dielectric and semiconductor distributed
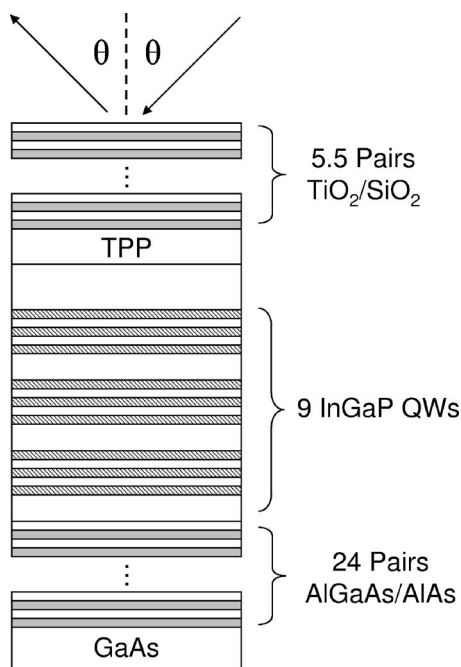
FIG. 1. The organic-inorganic semiconductor microcavity structure used to observe strong coupling between Frenkel and Wannier-Mott excitons through their mutual interaction with a common cavity mode.

Bragg reflectors (DBRs). The QWs were placed in sets of three at the electric field antinodes of the structure to maximize the interaction between the cavity photon and the QW exciton. The bottom DBR mirror consists of a 24-pair DBR composed of undoped $Al_{0.46}Ga_{0.54}As$ ($n_{AlGaAs}=3.45$) and AlAs ($n_{AlAs}=3.04$), grown by gas source molecular beam epitaxy (GSMBE), on a (100) GaAs substrate. Following this, nine 12-nm-thick $In_{0.52}Ga_{0.48}P$ QWs with 12.5-nm-thick $(Al_{0.4}Ga_{0.6})In_{0.5}P$ barriers were similarly grown to form the inorganic active region. A 320-nm-thick layer of TPP was deposited on a room temperature substrate onto the (AlGa)InP spacer layer by vacuum thermal sublimation in a chamber with a base pressure of approximately 10^{-7} Torr. The deposition conditions result in highly polycrystalline films. The (AlGa)InP spacer thickness (75 nm) is sufficient to prevent Förster energy transfer between the QWs and TPP.[19] To complete the structure, a 5.5 pair DBR consisting of TiO_2 ($n_{TiO_2}=2.30$) and SiO_2 ($n_{SiO_2}=1.46$) was deposited on top of the TPP by rf magnetron sputtering. Angularly resolved reflectivity spectra for the full organic-inorganic microcavity were collected as a function of temperature under white light excitation through the TiO_2/SiO_2 DBR stack.[20]

The refractive index profile and the spatial variation of the optical field intensity within the microcavity are shown in Fig. 2. The spacing and placement of the InGaP quantum well sets were optimized to provide maximum overlap between the QWs and the optical field profile.

To understand the nature of the Wannier-Mott polariton states, an inorganic microcavity was also fabricated by first growing the AlGaAs/GaAs DBR, followed by the InGaP MQW structure. The sample was capped by depositing a dielectric mirror [seven pairs of SiN_x ($n_{SiN_x}=2.10$) and SiO_2
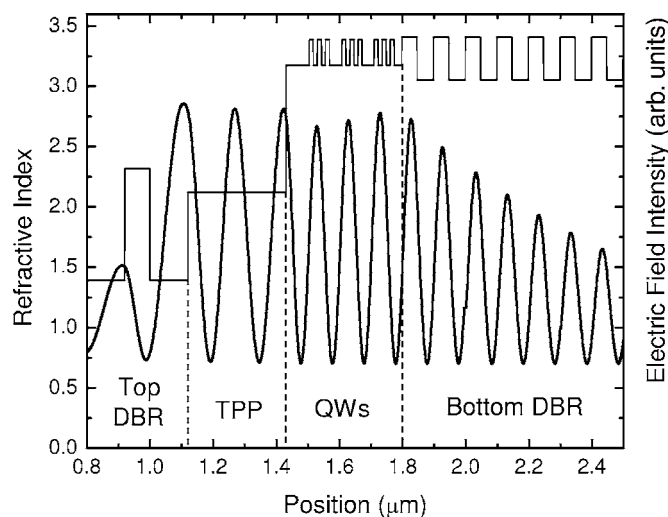

FIG. 2. The refractive index profile and calculated electric field intensity distribution (normal incidence) in the structure of Fig. 1.

($n_{SiO_2}=1.46$)] on top of the inorganic QW structure by plasma-enhanced chemical vapor deposition. Angularly resolved reflectivity spectra were collected through the SiN_x/SiO_2 DBR stack.

III. RESULTS

Quantum wells comprised of InGaP are a suitable partner for TPP ($E_{Frenkel}=1.90\pm0.02$ eV, measured at 300 K), given their heavy-hole excitonic absorption in the red at $E_{Wannier-Mott}=(1.972\pm0.002)$ eV at 4 K. Figure 3 shows the absorbance spectrum of TPP at room temperature, as well as the reflectivity spectrum of the inorganic component of the hybrid microcavity structure at an angle of 65° at 4 K. The
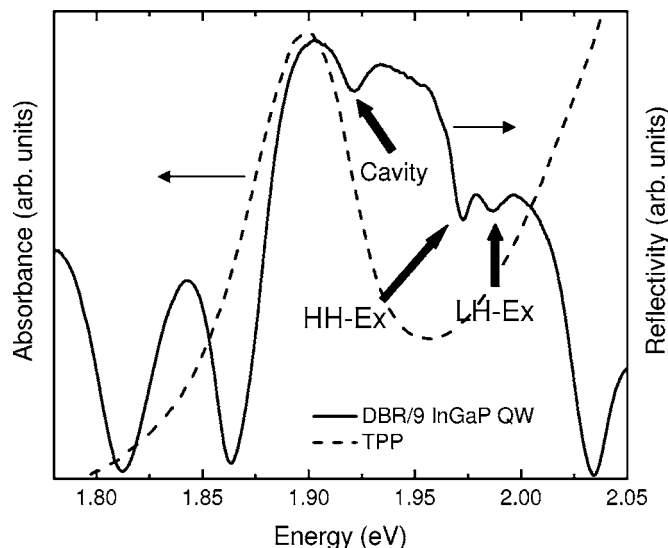

FIG. 3. The room temperature absorbance of tetraphenylporphyrin, and the low-temperature (4 K) reflectivity of the inorganic InGaP/(AlGa)InP quantum well component of the hybrid structure at an angle of 65°. Excitonic absorption features in the inorganic quantum wells are denoted by solid arrows.
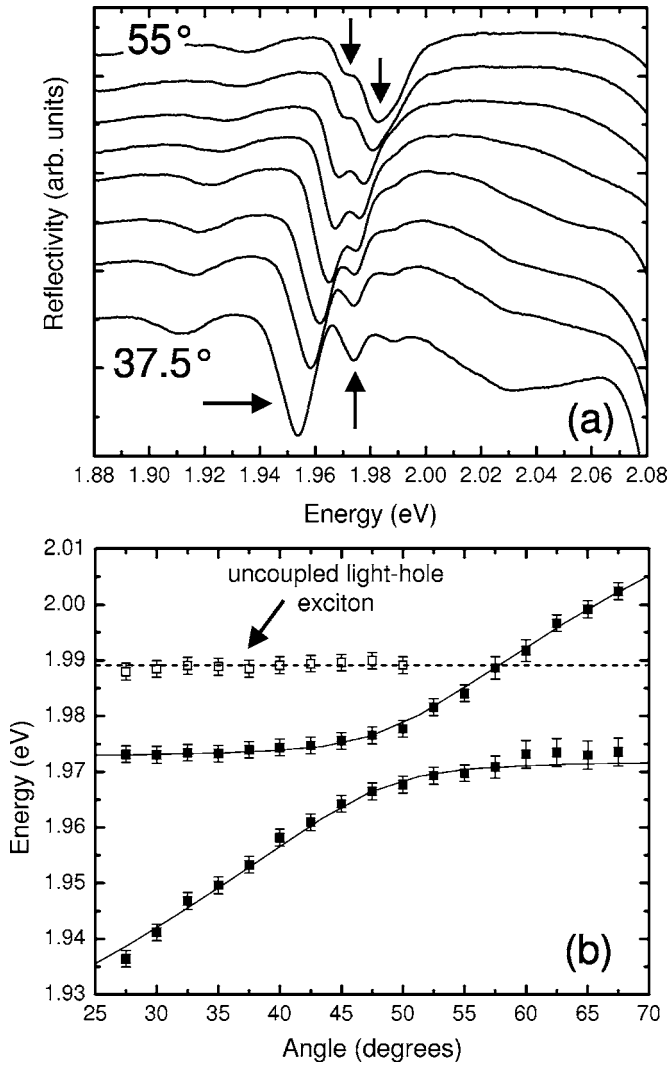
FIG. 4. (a) Reflectivity spectra at 4 K from an InGaP/(AlGa)InP semiconductor quantum well microcavity structure for angles of incidence ranging from 37.5° to 55°. The arrows denote features resulting from the strong coupling of the cavity mode and the heavy-hole exciton transition of InGaP at $E_{\text{Wannier-Mott}}=1.972$ eV. (b) The dispersion relation extracted from the reflectivity spectra of (a). The fits (solid lines) are obtained using a coupled oscillator model (see text) with a splitting of $\Omega_{\text{InGaP}}=10$ meV.
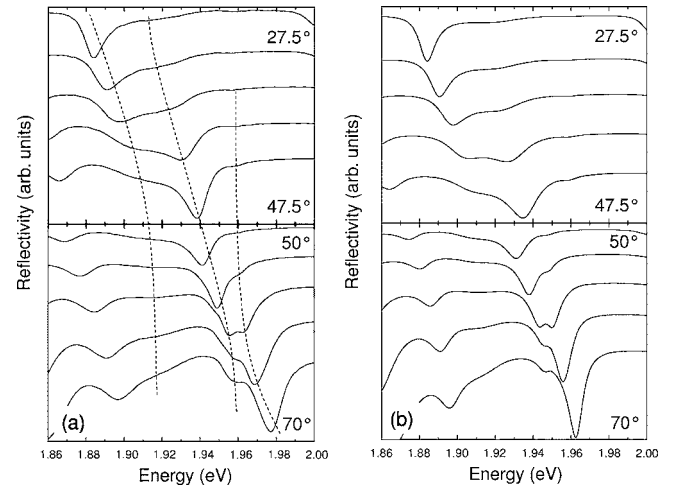

FIG. 5. (a) Reflectivity spectra at 100 K for the hybrid organic-inorganic semiconductor microcavity structure of Fig. 1. The three-body coupling between the Frenkel and Wannier-Mott excitons and the cavity mode is denoted by the broken lines. (b) Transfer matrix simulations of the reflectivity of the hybrid organic-inorganic microcavity structure in Fig. 1. Qualitative agreement is obtained with the experimental spectra of (a).

stop band of the AlGaAs/AlAs DBR is clearly visible from 1.86 eV to 2.03 eV, as are three separate dips in the reflectivity spectrum. The large dip centered in the DBR stopband is a weak cavity mode resulting from reflection between the AlGaAs/AlAs DBR and the spacer/air interface. The two smaller dips on the high-energy side of the DBR correspond to heavy-hole and light-hole excitonic absorption. Previous work has demonstrated that TPP can effectively form polaritons in an optical microcavity at room temperature.[14]

As a precursor to the study of the hybrid structure, the angularly resolved reflectivity of a purely inorganic microcavity was measured at 4 K [see Fig. 4(a)]. The resulting dispersion curve is shown in Fig. 4(b) and is fit using a coupled oscillator model. To our knowledge, there has been no report on the use of the red-emitting InGaP as an active material for strongly coupled devices.

Angularly resolved reflectivity spectra collected at 100 K for the full hybrid organic-inorganic structure are shown in Fig. 5(a). In the transfer matrix simulations of Fig. 5(b), the Wannier-Mott excitonic transition of InGaP is modeled as a Lorentzian oscillator[1] with a heavy hole oscillator strength of $f_{\text{hh}}=4.9\times10^{12}$ cm^{-2}, a full width at half maximum (FWHM) of $\gamma_{\text{hh}}=7$ meV, a background dielectric constant of $\varepsilon_b=11.5$, and a center transition energy of 1.957 eV. The values of f_{hh} and γ_{hh} are determined by fitting the transfer matrix simulation to reflectivity spectra collected from the inorganic-only structure of Fig. 4 as well as the hybrid structure of Fig. 5(a). The Frenkel excitonic transition of TPP is modeled using a peak absorbance of $\alpha=2.8\times10^4$ cm^{-1}, $\gamma_{\text{TPP}}=42$ meV, a background index of refraction of $n_{\text{TPP}}=2.12$, and a center transition energy of 1.917 eV. The values of α and γ_{TPP} were determined from low-temperature transmission measurements made on a film of TPP deposited on a quartz substrate.

In cases where the Rabi splitting is comparable to the polaritonic linewidth, absorbance measurements (A) are favored over reflectivity (R) as the most quantitative measure of strong exciton-photon coupling.[1,21] In the hybrid organic-inorganic microcavity studied here, the structure is purposely unbalanced, with the reflectivity of the AlGaAs/AlAs back mirror exceeding that of the TiO$_2$/SiO$_2$ front mirror. This imbalance leads to the transmission, $T\ll R$ for this structure on resonance, such that the absorbance is $A\sim1-R$. Transmission spectra were calculated for the hybrid structure as a function of angle using transfer matrices, and in all cases $T<1\%$ on resonance. This result further validates the use of reflectivity measurements in Fig. 5(a) to examine the strongly coupled state.
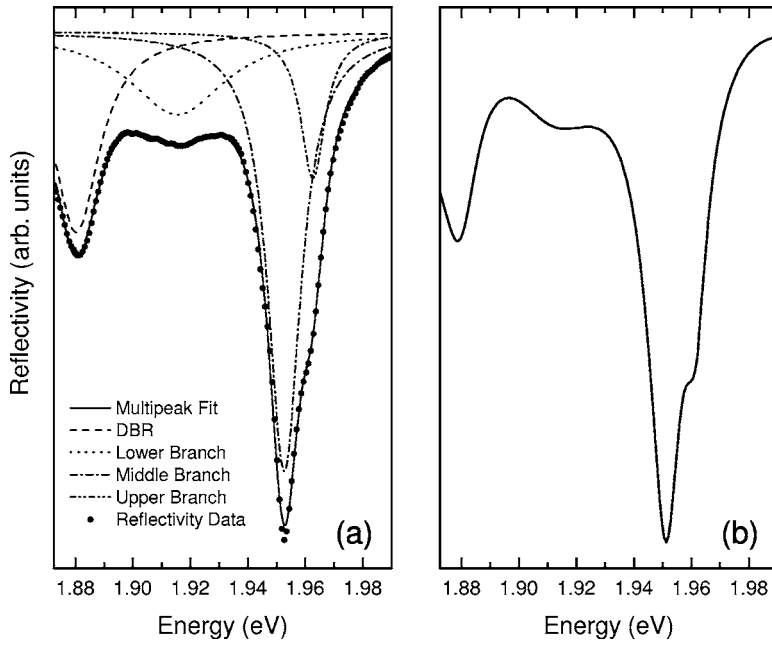
FIG. 6. (a) Measured reflectivity spectrum at 100 K at an angle of 57.5°. Also shown is the multiple Lorentzian function deconvolution of the spectrum used to extract the peak positions of each feature. Some raw data points have been omitted in order to increase the visibility of the Lorentzian fits. (b) Simulated reflectivity spectrum at the same angle. All three coupled features are clearly visible in both the measured and simulated spectra.

IV. DISCUSSION

In Fig. 4(a), a clear anticrossing is observed that results from strong coupling between the cavity photon and the heavy-hole excitonic transition of the InGaP QWs at 4 K. The resulting dispersion [Fig. 4(b)] can be modeled using coupled oscillators with a cavity cutoff energy E_0 =1.920 eV, an average cavity refractive index of 3.27, and a splitting of Ω_{InGaP}=10 meV. The uncoupled light-hole excitonic transition is also observed in the reflectivity spectra of Fig. 4(a), and is included in the dispersion curve.

In the hybrid structure, three separate features are observed in reflectivity at 100 K [Fig. 5(a)]. For small angles ($\theta < 47.5°$), two features dominate the spectra and show a pronounced anticrossing. These features result from strong coupling between the Frenkel exciton and the cavity mode. As the angle of incidence is further increased, a third feature emerges near the excitonic resonance of the inorganic QWs, and all three features anticross with increasing angle of incidence. For these intermediate angles ($47.5° < \theta < 60°$), the two excitons of the system are mixed with each other, and with the cavity photon. The positions of the three coupled features are denoted by the broken lines in Fig. 5(a). At large angles ($\theta > 60°$), two features dominate the spectrum, namely, coupling between the Wannier-Mott exciton and the cavity mode. The polaritonic linewidths observed at high angles are significantly narrower than those encountered at low angles because the uncoupled Wannier-Mott exciton linewidth is much narrower than that of the uncoupled Frenkel exciton (see Fig. 3).

Figure 5(b) shows transfer matrix simulations of the reflectivity at angles of incidence corresponding to those in Fig. 5(a). In these simulations, both excitons are modeled as Lorentz oscillators using the parameters discussed in Sec. III. The simulations qualitatively agree with experimental data. Slight discrepancies result from uncertainties in the low-temperature refractive indices used in the calculation.

Figures 6(a) and 6(b) compare in detail the experimental data collected at 100 K at an angle of 57.5° with the simulated reflectivity spectrum at the same angle, respectively. All three coupled features are clearly visible in both spectra. In Fig. 6(b), the multiple Lorentzian function deconvolution of the spectrum used to extract the peak positions of each feature is also shown. Lorentzian functions were used to fit and extract the peak centers of each feature in the reflectivity spectra of Fig. 5(a) as functions of the angle of incidence.

For a microcavity with coupling between a cavity photon, and Frenkel and Wannier-Mott excitons, the dispersion relation is modeled as a three-body coupled oscillator,[4–6,22]

$$\begin{bmatrix} E_p & V_{\text{Frenkel}} & V_{\text{Wannier-Mott}} \\ V_{\text{Frenkel}} & E_{\text{Frenkel}} & 0 \\ V_{\text{Wannier-Mott}} & 0 & E_{\text{Wannier-Mott}} \end{bmatrix} \begin{bmatrix} \alpha \\ \beta \\ \gamma \end{bmatrix} = \varepsilon \begin{bmatrix} \alpha \\ \beta \\ \gamma \end{bmatrix}, \quad (1)$$

where α, β, and γ are the mixing coefficients of the new eigenvectors of the strongly coupled system. Here, two interaction potentials ($V_{\text{Frenkel}}, V_{\text{Wannier-Mott}}$) are included in the Hamiltonian, as are the two uncoupled exciton energies ($E_{\text{Frenkel}}, E_{\text{Wannier-Mott}}$). The cavity photon dispersion, E_p, can be expressed in terms of the angle of incidence as $E_p = E_0(1 - \sin^2 \theta/n^2)^{-1/2}$, where E_0 is the cutoff energy and n is the cavity index of refraction.[8]

The dispersion relations for the hybrid structure are shown in Figs. 7(a) and 8(a) for temperatures of 100 K and 4 K, respectively. For the dispersion of Fig. 7(a), the energy eigenvalues (ε) were determined numerically using Eq. (1), where E_0=1.861 eV, E_{Frenkel}=1.917 eV, $E_{\text{Wannier-Mott}}$ =1.957 eV, n=2.79, V_{Frenkel}=10 meV, and $V_{\text{Wannier-Mott}}$ =4 meV. The dispersion curve at 4 K [Fig. 8(a)] is fit using E_0=1.865 eV, E_{Frenkel}=1.918 eV, $E_{\text{Wannier-Mott}}$=1.970 eV, n =2.81, V_{Frenkel}=11 meV and $V_{\text{Wannier-Mott}}$=4 meV. The value of the interaction potential, $V_{\text{Wannier-Mott}}$=4 meV, is consistent with that of $\Omega_{\text{InGaP}}/2$=5 meV obtained from the inorganic InGaP microcavity of Fig. 4. The uncoupled Frenkel
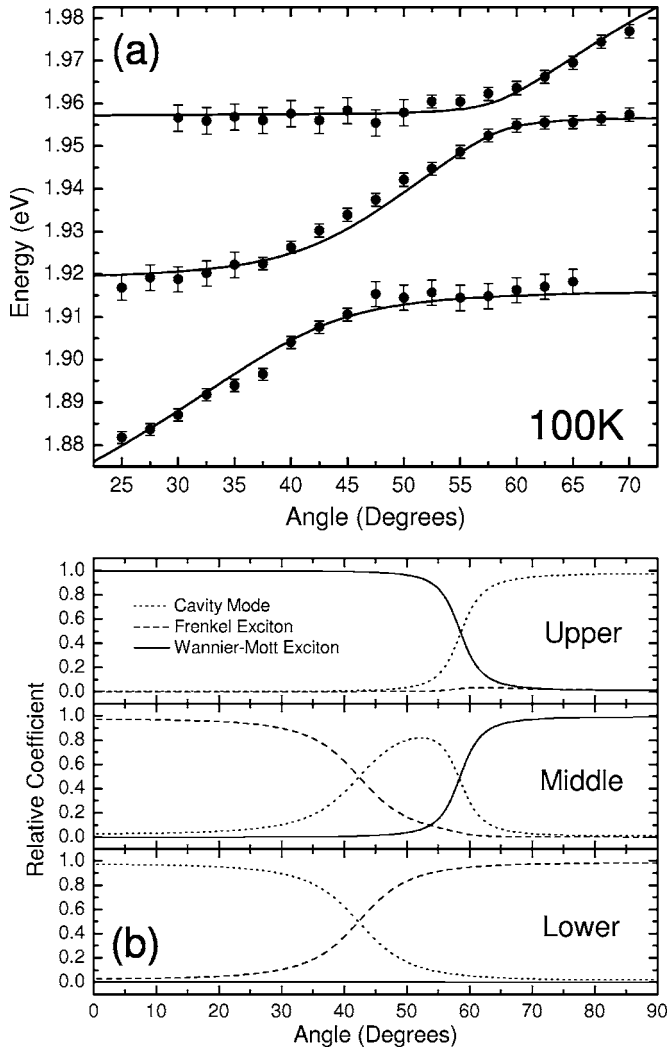
FIG. 7. (a) Dispersion relation extracted from the reflectivity spectra of Fig. 5. The pronounced anticrossings result from strong coupling to both the organic Frenkel exciton and the inorganic Wannier-Mott exciton. A three-body coupled oscillator model (solid lines) yields interaction potentials of $V_{\text{Frenkel}}=10$ meV and $V_{\text{Wannier-Mott}}=4$ meV. (b) Mixing coefficients $|\alpha|^2$, $|\beta|^2$, and $|\gamma|^2$ extracted from the fits of (a). The middle branch shows significant mixing between both the Frenkel and Wannier-Mott excitons and the cavity photon.

exciton energy used in the fit is blue-shifted in comparison to its value at room temperature. This shift is consistent with temperature-dependent transmission measurements separately performed on films of TPP deposited on quartz substrates. The uncoupled Wannier-Mott energy used in the fit agrees with the value determined from Fig. 3.

In Fig. 7(b), the mixing coefficients $|\alpha|^3$, $|\beta|^2$, and $|\gamma|^2$ [from Eq. (1)] are plotted versus angle for each branch of the hybrid dispersion relation of Fig. 7(a). The lower polariton branch [bottom, Fig. 7(b)] has symmetrically varying amounts of cavity photon and Frenkel exciton character. The middle polariton branch exhibits significant mixing between the cavity photon and both excitons with the point of strongest coupling occurring at $\theta \sim 54°$, where the branch character consists of equal parts Frenkel and Wannier-Mott
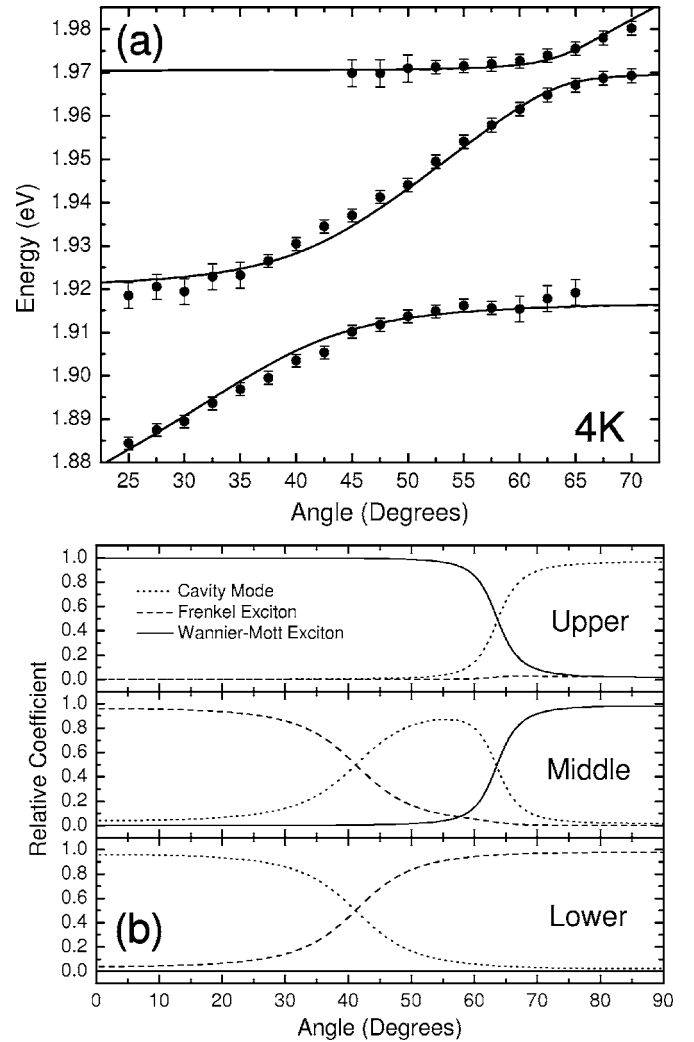
FIG. 8. (a) Dispersion relation obtained for the hybrid structure of Fig. 1 at temperature of 4 K. A three-body coupled oscillator model (solid lines) yields interaction potentials of $V_{\text{Frenkel}}=11$ meV and $V_{\text{Wannier-Mott}}=4$ meV. (b) Mixing coefficients $|\alpha|^2$, $|\beta|^2$, and $|\gamma|^2$ extracted from the fits of (a).

($\sim 10\%$), and $\sim 80\%$ cavity photon [middle, Fig. 7(b)]. In the upper branch, mixing is observed between the cavity photon and the Wannier-Mott excitonic resonance [top, Fig. 7(b)], and at large angles some mixing of the Frenkel exciton also occurs as a result of the strong coupling between the cavity and the Frenkel state.

At 4 K, the absorbance of the InGaP QWs is blue-shifted, and hence we expect a reduction in the mixing between the two excitonic states. Indeed, the exciton hybridization of the middle branch in the hybrid structure is weaker at 4 K than at 100 K, with the branch character consisting of equal parts Frenkel and Wannier-Mott ($\sim 7\%$), and $\sim 86\%$ cavity photon, as shown in Fig. 8(b). For temperatures above 100 K, the three-body coupling becomes increasingly difficult to resolve since the linewidth of the Wannier-Mott exciton becomes comparable to the splitting between the middle and the upper branches.

V. CONCLUSION

We have demonstrated strong exciton-photon coupling between the Frenkel exciton of an organic semiconductor and the Wannier-Mott exciton of inorganic QWs through their mutual interaction with a cavity photon. The hybridized exciton-polariton state is modeled as a three-body coupled oscillator. Hybrid Frenkel-Wannier-Mott polaritonic states are expected to exhibit nonlinear optical behavior that draws on the properties of both component excitons. Namely, this unusual eigenstate has been predicted to possess the large exciton oscillator strength of a molecular Frenkel exciton and the low saturation density typical of inorganic Wannier-Mott excitons.[17] In addition, the hybrid state may provide a path for exciting the organic polariton by either optical or electrical means.[18] This is especially significant as there has yet to be a successful demonstration of an electrically pumped organic laser. In addition to being useful in the design of unique optoelectronic devices, hybrid states provide an opportunity to study the storage and transfer of energy between different excitonic species.

*Present address: Department of Chemical Engineering and Materials Science, University of Minnesota, Minneapolis, Minnesota 55455, USA.

†Author to whom correspondence should be addressed. Email address: stevefor@umich.edu

[1] V. Savona, L. C. Andreani, P. Schwendimann, and A. Quattropani, Solid State Commun. **93**, 733 (1995).

[2] C. Weisbuch, M. Nishioka, A. Ishikawa, and Y. Arakawa, Phys. Rev. Lett. **69**, 3314 (1992).

[3] R. Houdre, R. P. Stanley, and M. Ilegems, Phys. Rev. A **53**, 2711 (1996).

[4] R. J. Holmes and S. R. Forrest, Phys. Rev. Lett. **93**, 186404 (2004).

[5] D. G. Lidzey, D. D. C. Bradley, A. Armitage, S. Walker, and M. S. Skolnick, Science **288**, 1620 (2000).

[6] J. Wainstain, C. Delalande, D. Gendt, M. Voos, J. Bloch, V. Thierry-Mieg, and R. Planel, Phys. Rev. B **58**, 7269 (1998).

[7] P. G Lagoudakis, M. D. Martin, J. J. Baumberg, G. Malpuech, and A. Kavokin, J. Appl. Phys. **95**, 2487 (2004).

[8] M. S. Skolnick, T. A. Fisher, and D. M. Whittaker, Semicond. Sci. Technol. **13**, 645 (1998).

[9] D. G. Lidzey, D. D. C. Bradley, M. S. Skolnick, T. Virgili, S. Walker, and D. M. Whittaker, Nature (London) **395**, 53 (1998).

[10] D. G. Lidzey, D. D. C. Bradley, T. Virgili, A. Armitage, M. S. Skolnick, and S. Walker, Phys. Rev. Lett. **82**, 3316 (1999).

[11] N. Takada, T. Kamata, and D. D. C. Bradley, Appl. Phys. Lett. **82**, 1812 (2003).

[12] P. Schouwink, H. von Berlepsch, L. Dahne, and R. F. Mahrt, J. Lumin. **94-95**, 821 (2001).

[13] J. R. Tischler, M. S. Bradley, V. Bulovic, J.-H. Song, and A. Nurmikko, Phys. Rev. Lett. **95**, 036401 (2005).

[14] R. J. Holmes and S. R. Forrest, Phys. Rev. B **71**, 235203 (2005).

[15] E. Goobar, R. J. Ram, J. Ko, G. Bjork, M. Oestreich, and A. Imamoglu, Appl. Phys. Lett. **69**, 3465 (1996).

[16] D. G. Lidzey, J. Wenus, D. M. Whittaker, G. Itskos, P. N. Stavrinou, D. D. C. Bradley, and R. Murray, J. Lumin. **110**, 347 (2004).

[17] V. M. Agranovich, D. M. Basko, G. C. La Rocca, and F. Bassani, J. Phys. Condens. Matter **10**, 9369 (1998).

[18] V. M. Agranovich, H. Benisty, and C. Weisbuch, Solid State Commun. **102**, 631 (1997).

[19] V. M. Agranovich, D. M. Basko, G. C. La Rocca, and F. Bassani, Synth. Met. **116**, 349 (2001).

[20] R. Houdre, C. Weisbuch, R. P. Stanley, U. Oesterle, P. Pellandini, and M. Ilegems, Phys. Rev. Lett. **73**, 2043 (1994).

[21] R. Houdre, Phys. Status Solidi B **242**, 2167 (2005).

[22] A. Armitage, M. S. Skolnick, A. Kavokin, D. M. Whittaker, V. N. Astratov, G. A. Gehring, and J. S. Roberts, Phys. Rev. B **58**, 15367 (1998).